Molecular Imaging of *HER2*-Expressing Malignant Tumors in Breast Cancer Patients Using Synthetic ^{111}In- or ^{68}Ga-Labeled Affibody Molecules

Richard P. Baum[1], Vikas Prasad[1], Dirk Müller[1], Christiane Schuchardt[1], Anna Orlova[2,3], Anders Wennborg[2], Vladimir Tolmachev[2,3], and Joachim Feldwisch[2,3]

[1]Zentralklinik Bad Berka GmBH, PET-Zentrum, Bad Berka, Germany; [2]Affibody AB, Stockholm, Sweden; and [3]Department of Oncology, Radiology and Clinical Immunology, Rudbeck Laboratory, Uppsala University, Uppsala, Sweden

The clinical utility of a human epidermal growth factor receptor 2 (*HER2*)–targeting Affibody molecule for detection and characterization of *HER2*-positive lesions was investigated in patients with recurrent metastatic breast cancer. **Methods:** Three patients received ^{111}In- or ^{68}Ga-labeled DOTA^0-Z$_{HER2:342\text{-}pep2}$ (ABY-002). γ-Camera, SPECT, or PET/CT images were compared with earlier ^{18}F-FDG PET/CT results. **Results:** Administration of radiolabeled ABY-002 was well tolerated. Blood kinetics of radiolabeled ABY-002 showed a first half-life of 4–14 min, second half-life of 1–4 h, and third half-life of 12–18 h. Radiolabeled ABY-002 detected 9 of 11 ^{18}F-FDG–positive metastases as early as 2–3 h after injection. **Conclusion:** Molecular imaging using ^{111}In- or ^{68}Ga-labeled ABY-002 has the potential to localize metastatic lesions in vivo, adds qualitative information not available today by conventional imaging techniques, and may allow the *HER2* status to be determined for metastases not amenable to biopsy. To our knowledge, this is the first report on clinical imaging data obtained with a non–immunoglobulin-based scaffold protein.

Key Words: diagnostic imaging; breast cancer; PET/CT; ^{111}In; ^{68}Ga

J Nucl Med 2010; 51:892–897
DOI: 10.2967/jnumed.109.073239

Functional imaging with SPECT or PET is used to characterize biologic processes at the molecular level. Most of these investigations are performed using ^{18}F-FDG PET, which has proven value for the detection of metastatic and recurrent disease and early treatment response (*1,2*). However, ^{18}F-FDG PET shows increased glucose metabolism without providing information on the presence of cancer-specific cell-surface receptors and therefore does not provide guidance for receptor-targeted therapy.

Received Nov. 26, 2009; revision accepted Feb. 17, 2010.
For correspondence or reprints contact: Joachim Feldwisch, Affibody AB, Lindhagensgatan 133, SE-112 51 Stockholm, Sweden.
E-mail:joachim.feldwisch@affibody.com

The human epidermal growth factor receptor 2 (*HER2*) is overexpressed in several cancer types characterized by more aggressive tumors and decreased overall survival but is limited or absent in normal adult tissue (*3*). Determining the presence of *HER2* in potentially responsive patients is increasingly important given the growing arsenal of *HER2*-targeted therapies (*4*). Diagnosis of *HER2* overexpression is recommended for all newly diagnosed breast carcinomas (*5,6*). However, approximately 10%−20% of current *HER2* assessments may be inaccurate. Thus, some eligible patients do not receive *HER2*-targeted therapy whereas others are exposed to unnecessary therapy (*6,7*).

Discordance in *HER2* expression between the primary tumor and metastases complicates diagnosis of recurrent disease (*8,9*). Thus, a complementary in vivo diagnostic method might be beneficial for improved prediction and monitoring of therapy response—for example, a molecular imaging agent with high specificity and affinity for *HER2,* enabling detection and localization of all *HER2*-positive tumor lesions, including those not amenable to biopsy.

Affibody molecules (Affibody AB), small non–immunoglobulin-affinity proteins, are proven tracers for molecular imaging (*10*). Preclinical characterization of the ^{111}In-labeled Affibody molecule DOTA^0-Z$_{HER2:342\text{-}pep2}$ (ABY-002) in mice showed specific tumor targeting and allowed imaging as soon as 1 h after injection (*11*).

Here we describe the first in-humans administration of ^{111}In-ABY-002 and ^{68}Ga-ABY-002 in patients with recurrent breast cancer.

MATERIALS AND METHODS

The 58-amino-acid long peptide ABY-002 was synthesized (Bachem) and labeled with ^{111}In or ^{68}Ga at a good-manufacturing-practice–certified radiopharmacy (Zentral Klinik Bad Berka). Three patients with recurrent metastatic breast cancer and known lesions identified by CT or ^{18}F-FDG PET/CT received approximately 80–90 μg of ABY-002. The exploratory research was approved by the local ethics committee. Patients were imaged

TABLE 1. Patient Characteristics and Imaging Schedules

Characteristic	Patient 1	Patient 2	Patient 3
Age at imaging (y)	64	39	58
TNM classification	pT_2 pN_1 M_x	pT_{1c} $pN_{1a(2/11)}$ M_0, L_0, V_0, R_0	pT_2 pN_0 M_0
Grade	G2–3	G3	G2
Receptor status at diagnosis	ER/PR-positive	ER/PR-negative	ER/PR-negative
Tumor marker		Ki-67, 20%	
HER2 status at diagnosis	Not analyzed	3+	3+
Trastuzumab treatment	Not before ABY-002 imaging	Not before ABY-002 imaging	Ongoing at time of ABY-002 imaging
^{18}F-FDG PET/CT	Day 0	Day 0	Day 0
Dose	293 MBq	284 MBq	278 MBq
Whole-body PET/CT	90 min after injection	95 min after injection	85 min after injection
^{111}In-ABY-002	Day 35		Day 13
Dose	123 MBq		101.3 MBq
Dynamic scan	1–30 min		
WBS	1, 2, 4, and 72 h after injection		2, 4, and 20 h after injection
SPECT	3 h after injection		20 h after injection
^{68}Ga-ABY-002	Day 74	Day 19	Day 14
Dose	110 MBq	187 MBq	267 MBq
Whole-body PET/CT	90 and 250 min after injection	95 min after injection	135 min after injection

ER/PR = estrogen receptor/progesterone receptor.
Last ^{18}F-FDG PET/CT scan was set as day 0.

between November 2005 and April 2006 in accordance with the German regulations concerning administration of radiolabeled substances to humans. Details about the radiolabeling and imaging are described in the supplemental materials (available online only at http://jnm.snmjournals.org).

RESULTS

Three breast cancer patients received radiolabeled ABY-002. Two patients received both ^{111}In-ABY-002 and ^{68}Ga-ABY-002, and 1 patient received ^{68}Ga-ABY-002 only. The 5 administrations (in total) of ^{111}In-ABY-002 or ^{68}Ga-ABY-002 were well tolerated. No acute adverse drug reactions and no clinically significant changes in blood pressure or pulse occurred during a follow-up period of 3 h after injection. Patient characteristics are summarized in Tables 1 and 2.

Patient 1 was diagnosed with mammary carcinoma 11 y earlier. The *HER2* status of the primary tumor was unknown, and the patient had not been treated with trastuzumab before the ^{111}In-ABY-002 SPECT investigation. A lymph node dissection in the left axilla performed 1 y earlier showed histologically 10 lymph node metastases with overexpression of *HER2* (HercepTest [DakoCytomation] score, 3+) in 60% of these nodes. One year after lymph node dissection, an ^{18}F-FDG PET/CT scan was obtained because of suspected progression of disease. One month after that scan, ^{111}In-ABY-002 was administered and its distribution was followed by dynamic scans for 30 min

TABLE 2. Standardized Uptake Value in Lesions on PET Scans of Patients 2 and 3

Site	Patient 2		Patient 3	
	^{18}F-FDG	^{68}Ga-ABY-002	^{18}F-FDG	^{68}Ga-ABY-002
Region of liver metastasis	9.0	18.2 (surrounding normal liver, 15.6–18.2)		
Left iliac spine			8.6	2.5
Soft tissue close to iliac bone			8.6	4.3
Acetabulum/femur head			8.6	2.1
Sartorius muscle			3.7	2.4
Potential lymphangiosis within quadriceps muscle			4.8	2.6
Potential chest wall lesion				1.6

(Supplemental Fig. 1). The subclavian vein and the blood pool radioactivity in the heart were visible on the 1-min image but not on later images. The left kidney and the liver could be identified after 2 min. Image intensity increased until 5 min and remained constant for the remaining 25 min. Whole-body scans, performed at 1, 2, and 4 h after injection, showed strong uptake of radioactivity in the liver and kidneys and weak uptake in the gastrointestinal tract and in the parotid and submandibular glands. At 2 and 4 h after injection, additional uptake of radioactivity was visible in the mediastinum and the lateral left thorax (Fig. 1). High-quality SPECT images were obtained 3 h after injection, enabling detection of 3 lymph node metastases in the anterior left mediastinum (near the aortic arch, paraaortally and retrosternally) and a small (diameter, 12–14 mm) lesion within the latissimus dorsi muscle at the lateral left thorax. Biopsy and HercepTest analysis of the latter confirmed a *HER2* score of 3+. The same 4 lesions were detected by ^{18}F-FDG PET/CT (Fig. 1). An additional lesion identified by ^{18}F-FDG PET/CT and interpreted as either lymph node or adrenal metastasis was not resolved by ^{111}In-ABY-002 imaging because of overlying radioactivity in the left kidney.

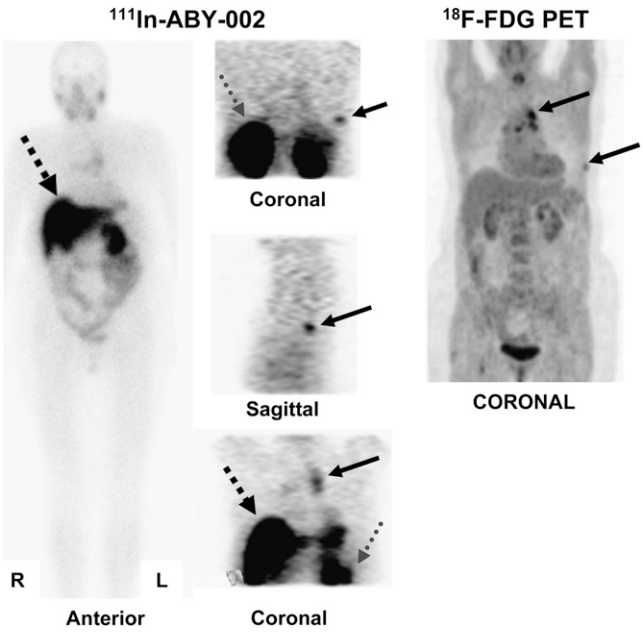

FIGURE 1. Images of patient 1 showing localization of metastases (solid arrows), kidney (dotted arrows), and liver (dashed arrows). γ-camera imaging was performed after intravenous injection of 123 MBq of ^{111}In-ABY-002 with peptide mass dose of less than 100 μg. Whole-body scan 4 h after injection (left) shows uptake predominantly in liver and kidney, with additional uptake in parotid and submandibular glands, thorax, and gastrointestinal tract. SPECT images 3 h after injection (middle) show the localization of thoracic wall metastasis (upper coronal image and sagittal image) and mediastinal lymph node metastases (lower coronal image). Findings indicate *HER2*-positive metastases in mediastinal lymph nodes and thoracic wall, as was confirmed for the thoracic wall metastasis by HercepTest score of 3+. PET was performed after intravenous injection of 293 MBq of ^{18}F-FDG. Coronal maximum-intensity-projection image 90 min after injection (right) shows localization of thoracic wall metastasis and mediastinal lymph node metastases.

After surgical resection of the thoracic wall metastasis and chemotherapy with 2 doses of vinorelbine (30 mg/m^2/d at 19 and 26 d after ^{111}In-ABY-002 imaging), none of these lesions were visible by ^{68}Ga-ABY-002 PET/CT performed 39 d later. This finding is consistent with the significant reduction of the 2 tumor markers carcinoembryonic antigen (cutoff, 3.4) and CA 15-3 (cutoff, <25), which fell from 8.2 ng/mL and 83.3 U/mL, respectively, before therapy to 4.8 ng/mL and 43.4 U/mL, respectively, on the day of imaging.

Patient 2 was diagnosed with *HER2*-positive mammary carcinoma 18 mo earlier. ^{18}F-FDG uptake was observed in 1 liver metastasis and in a mediastinal lymph node (suggestive of a metastasis). ^{68}Ga-ABY-002 images could not provide unambiguous evidence of a *HER2* receptor–positive liver metastasis because of high background uptake of the tracer in the liver. The mediastinal lymph node showed no ^{68}Ga-ABY-002 uptake (a detailed description is provided in the supplemental material, including Supplemental Fig. 2).

Patient 3 was diagnosed 7 y earlier with *HER2*-positive breast cancer. Recurrent breast cancer with 5 hypermetabolic areas was identified by ^{18}F-FDG PET/CT. Of these, only the metastasis in the iliac spine could clearly be identified on CT. The soft-tissue metastasis could be identified on CT only in connection with the ^{18}F-FDG PET images, whereas the 3 other metastases were not identified on CT. MRI revealed changes in the sartorius muscle, but it was not possible to differentiate between changes based on inflammation and changes based on tumor infiltration. ^{111}In-ABY-002 SPECT 20 h after injection and ^{68}Ga-ABY-002 PET/CT approximately 2 h after injection clearly visualized the 5 lesions in the pelvic area (Fig. 2 and Supplemental Fig. 3). Comparison of the ^{68}Ga-ABY-002 and ^{18}F-FDG PET/CT images revealed 1 additional lesion in the right anterolateral chest wall near the axilla with increased ^{68}Ga-ABY-002 uptake but no hypermetabolic uptake of ^{18}F-FDG (Fig. 2A; Table 2).

Biopsies taken from the quadriceps muscle 4 mo later confirmed solid carcinoma metastasis. Histologically, the growth pattern was compatible with mammary carcinoma. More than 50% of the tumor cells showed a strong and mostly complete membrane staining for *HER2* (mean HercepTest score, 2+; minimal value, 0; maximal value, 3+).

At the time of imaging, the patient was on trastuzumab therapy and had a serum concentration of shed *HER2* extracellular domain in the range of about 40 ng/mL (40.5 ng/mL 1 mo before and 43.2 ng/mL at the time of imaging).

For all 3 patients, the blood kinetics of radiolabeled ABY-002 were assessed by following the radioactivity in blood from 2 min until 94 h (Fig. 3).

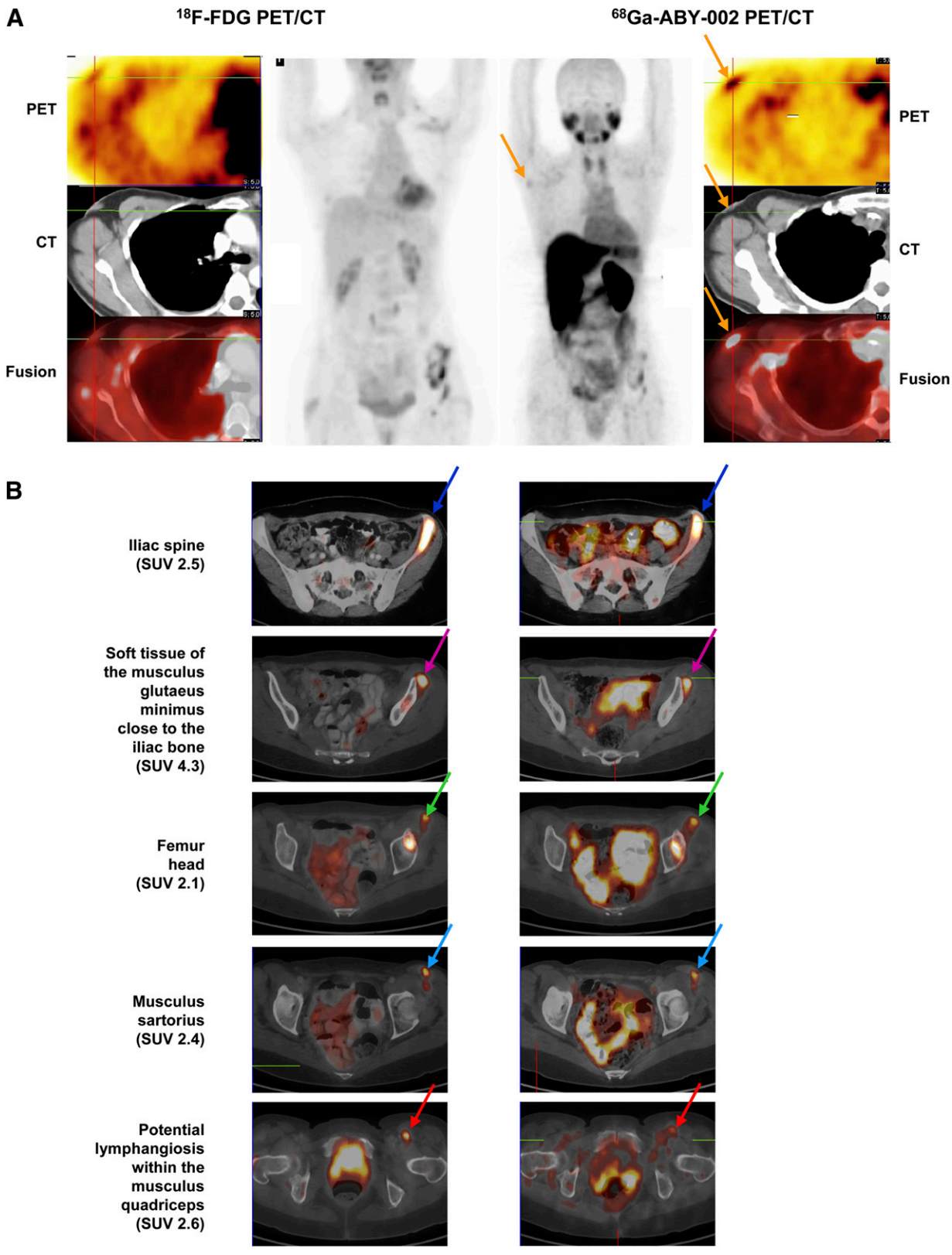

FIGURE 2. Images of patient 3 obtained 85 min after intravenous injection of 278 MBq of ^{18}F-FDG and 135 min after intravenous injection of 267 MBq of ^{68}Ga-ABY-002 with peptide mass dose of less than 100 μg. (A) Potential metastasis (arrows) in chest wall near the axilla is seen with ^{68}Ga-ABY-002 on transverse PET (top), CT (middle), and PET/CT (bottom) images and on coronal maximum-intensity-projection images (in between). This metastasis was not visible with ^{18}F-FDG. (B) ^{18}F-FDG (left column) and ^{68}Ga-ABY-002 (right column) transverse images of identified lesions (arrows) in pelvic area.

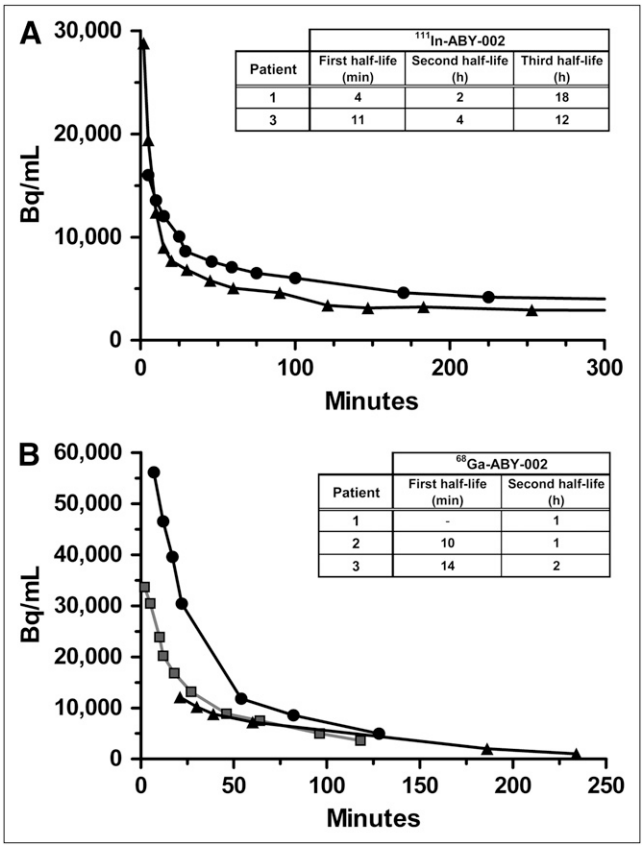

FIGURE 3. Blood kinetics in the 3 patients. Samples were collected at predetermined times after injection of radiolabeled ABY-002; radioactivity was measured with γ-counter (Isomed 2000; Nuklear Medizintechnik Dresden) and plotted over time; and values were applied for kinetic analysis using Origin Pro 7G (OriginLab) and exponential curve fit function ExpDec 1/2. (A) Blood kinetics of ^{111}In-ABY-002 in patients 1 (administered dose, 123 MBq [▲]) and 3 (101.3 MBq [●]). Time points between 22 and 94 h after injection are not included. (B) Blood kinetics of ^{68}Ga-ABY-002 in patients 1 (110 MBq [▲]), 2 (187 MBq [■]), and 3 (267 MBq [●]).

DISCUSSION

The presented results from 3 breast cancer patients demonstrate that the radiolabeled Affibody molecule ABY-002 has the potential to visualize *HER2*-expressing metastatic lesions in patients with metastatic breast cancer.

Analysis of the blood kinetics revealed rapid blood clearance of radiolabeled ABY-002 in humans with a first half-life of 4–11 min for ^{111}In-ABY-002 and 10–14 min for ^{68}Ga-ABY-002, in agreement with preclinical data on mice (*11*). The rapid kinetics enabled high-contrast SPECT or PET with radiolabeled ABY-002 to be performed in humans as soon as 2–3 h after injection. High uptake of radiolabeled ABY-002 was seen in the metastases, the kidneys, and the liver. Most of the previously identified lesions with ^{18}F-FDG PET/CT were visualized. Four of 5 known lesions in patient 1 were visualized with ^{111}In-ABY-002, and all 5 known lesions in patient 3 showed positive uptake of both ^{111}In-ABY-002 and ^{68}Ga-ABY-002. However, 2 lesions positive on ^{18}F-FDG PET/CT scans could not be visualized with radiolabeled ABY-002: 1 lesion in patient 1 and 1 lesion in patient 2. In patient 1, the known metastasis close to the kidney was not resolved with ^{111}In-ABY-002 because of overlying radioactivity in the kidney, and in patient 2 the liver metastasis was not resolved with ^{68}Ga-ABY-002 because of a high background level in surrounding nonmalignant liver tissue.

In patient 3, both ^{18}F-FDG and ^{68}Ga-ABY-002 improved the diagnosis of metastases because CT alone could not identify all the lesions. However, imaging with ^{68}Ga-ABY-002 added further information. The lesion in the sartorius muscle was differentially diagnosed as an inflammatory alteration or tumor infiltration by MRI. The ABY-002 images show overexpression of *HER2* indicating the presence of tumor tissue. This distinction could not be made with ^{18}F-FDG because both processes are associated with increased glucose uptake. Whereas glucose metabolism was equally elevated in both soft-tissue metastases and bone metastases, uptake of ^{68}Ga-ABY-002 was approximately 50% lower in bone metastases than in the soft-tissue lesion. One hypothesis is that the *HER2* expression level varies between metastases in different locations, possibly explaining the difference in hip-region SUVs, which ranged from 4.3 to 2.1 (50% lower). Although this observation is preliminary and in need of further validation, it could allow the use of ABY-002 to characterize different levels of *HER2* expression in tumors and to detect different degrees of response to receptor-targeted therapies. Recent preclinical data have demonstrated that this use of *HER2*-binding Affibody molecules is possible in mice bearing tumors with different *HER2* expression levels (*12*). The uptake of ABY-002 in a single potential lesion without significantly increased glucose metabolism is an interesting finding. Because biopsy data to confirm this potential receptor-versus-metabolism mismatch are not available, further clinical studies are warranted to validate this phenomenon.

Immunohistochemistry analysis (HercepTest) of 2 metastases amenable to surgery or biopsy confirmed that the lesions detected with radiolabeled ABY-002 were *HER2*-positive. The thoracic wall metastasis from patient 1 had a HercepTest score of 3+. Biopsies taken from the quadriceps muscle metastasis from patient 3 revealed heterogeneous *HER2* expression with scores ranging from 0 to 3+ and a mean score of 2+. Thus, the biopsy data provide additional support for the hypothesis that the difference in the standardized uptake values in the hip region could be due to heterogeneous *HER2* expression pattern in different lesions.

Adequate imaging results were obtained for patient 3 even though this patient was on trastuzumab therapy, confirming the extensive preclinical data that *HER2*-binding Affibody molecules—including ABY-002—and trastuzumab target separate epitopes on the extracellular domain

of *HER2* (*11,13*). Thus, potential interference from competitive target binding is not expected. A serum concentration of shed *HER2* extracellular domain in the range of about 40 ng/mL did not preclude tumor imaging.

One potential limitation is the high level of liver and kidney uptake seen with ^{111}In-ABY-002 and ^{68}Ga-ABY-002. Whereas high kidney uptake of radiolabeled ABY-002 was known from preclinical studies and is expected for a small protein with predominantly renal clearance, the liver uptake seen in patients was never observed in normal or tumor-bearing mice (*10,11*). One possible explanation could be that *HER2* expression in human liver leads to specific uptake although data on *HER2* expression in human liver are inconsistent (*14,15*).

The high detection rate of known lesions and the short time until the image acquisition after radiolabeled ABY-002 administration is in contrast to results from the few clinical studies performed with ^{111}In-diethylenetriaminepentaacetic acid (DTPA)-trastuzumab, ^{68}Ga-F(ab′)$_2$-trastuzumab, and ^{89}Zr-trastuzumab. ^{111}In-DTPA-trastuzumab was used in 3 studies aiming to identify patients at risk for trastuzumab-related cardiotoxicity (*16–18*). Only 45% of the known metastases were detected using ^{111}In-DTPA-trastuzumab (*17*). ^{68}Ga-F(ab′)$_2$-trastuzumab showed no uptake in 3 patients and showed measurable uptake in at least 1 lesion in 3 other patients with *HER2*-positive metastatic breast cancer, but multiple other lesions were not visualized (*19*). Recently, clinical application of ^{89}Zr-trastuzumab allowed detection of known and unknown lesions, with an optimal image-acquisition time point of 4–5 d after administration (*20*).

CONCLUSION

Imaging with ABY-002 seems to be well adapted for the clinical practice where tracer administration and image acquisition on the same day are preferred over modalities that extend over 2 or more days, such as is needed with antibodies or fragments thereof. Further clinical studies are warranted to assess the optimal time point, peptide and radioactivity doses for image acquisition, and sensitivity and specificity.

ACKNOWLEDGMENT

We thank Lars Abrahmsén for critically reading the manuscript.

REFERENCES

1. Brindle K. New approaches for imaging tumour responses to treatment. *Nat Rev Cancer.* 2008;8:94–107.
2. Baum RP, Prasad V. Molecular imaging for monitoring therapy response. In: Cook GJR, Maisey M-N, Britton KE, Chengazi V, eds. *Clinical Nuclear Medicine.* 4th ed. London: U.K.: Oxford University Press; 2007:57–79.
3. Press MF, Cordon-Cardo C, Slamon DJ. Expression of the HER-2/neu proto-oncogene in normal human adult and fetal tissues. *Oncogene.* 1990;5:953–962.
4. Murphy CG, Modi S. HER2 breast cancer therapies: a review. *Biologics.* 2009;3:289–301.
5. Molina R, Barak V, van Dalen A, et al. Tumor markers in breast cancer: European Group on Tumor Markers recommendations. *Tumour Biol.* 2005;26:281–293.
6. Wolff AC, Hammond ME, Schwartz JN, et al. American Society of Clinical Oncology/College of American Pathologists guideline recommendations for human epidermal growth factor receptor 2 testing in breast cancer. *J Clin Oncol.* 2007;25:118–145.
7. Tuma RS. Inconsistency of HER2 test raises questions. *J Natl Cancer Inst.* 2007;99:1064–1065.
8. Zidan J, Dashkovsky I, Stayerman C, Basher W, Cozacov C, Hadary A. Comparison of HER-2 overexpression in primary breast cancer and metastatic sites and its effect on biological targeting therapy of metastatic disease. *Br J Cancer.* 2005;93:552–556.
9. Tapia C, Savic S, Wagner U, et al. HER2 gene status in primary breast cancers and matched distant metastases. *Breast Cancer Res.* 2007;9:R31.
10. Tolmachev V. Imaging of HER-2 overexpression in tumors for guiding therapy. *Curr Pharm Des.* 2008;14:2999–3019.
11. Orlova A, Tolmachev V, Pehrson R, et al. Synthetic Affibody molecules: a novel class of affinity ligands for molecular imaging of HER2-expressing malignant tumors. *Cancer Res.* 2007;67:2178–2186.
12. Kramer-Marek G, Kiesewetter DO, Capala J. Changes in HER2 expression in breast cancer xenografts after therapy can be quantified using PET and ^{18}F-labeled Affibody molecules. *J Nucl Med.* 2009;50:1131–1139.
13. Kramer-Marek G, Kiesewetter DO, Martiniova L, Jagoda E, Lee SB, Capala J. [^{18}F]FBEM-$Z_{HER2:342}$-Affibody molecule: a new molecular tracer for in vivo monitoring of HER2 expression by positron emission tomography. *Eur J Nucl Med Mol Imaging.* 2008;35:1008–1018.
14. European Medicines Evaluation Agency. Trastuzumab scientific discussion. Available at: http://www.emea.europa.eu/humandocs/PDFs/EPAR/Herceptin/177400en6.pdf. Accessed March 18, 2010.
15. Human Protein Atlas. Version 5.0. Available at: http://www.proteinatlas.org. Accessed March 18, 2010.
16. Behr TM, Behe M, Wormann B. Trastuzumab and breast cancer. *N Engl J Med.* 2001;345:995–996.
17. Perik PJ, Lub-De Hooge MN, Gietema JA, et al. Indium-111-labeled trastuzumab scintigraphy in patients with human epidermal growth factor receptor 2-positive metastatic breast cancer. *J Clin Oncol.* 2006;24:2276–2282.
18. de Korte MA, de Vries EG, Lub-de Hooge MN, et al. ^{111}Indium-trastuzumab visualises myocardial human epidermal growth factor receptor 2 expression shortly after anthracycline treatment but not during heart failure: a clue to uncover the mechanisms of trastuzumab-related cardiotoxicity. *Eur J Cancer.* 2007;43:2046–2051.
19. Akhurst T, Morris PG, Modi S, et al. Positron emission tomography (PET) with radiolabeled F(ab′)2-trastuzumab fragments in patients (pts) with HER2-positive metastatic breast cancer (MBC): initial feasibility results. Poster presented at 2008 Breast Cancer Symposium; September 5–7, 2008; Washington, DC. Abstract 79.
20. Munnink TO, Dijkers E, Lub-de Hooge M, et al. HER-2-PET imaging with ^{89}Zr-trastuzumab in metastatic breast cancer patients [abstract]. *J Clin Oncol.* 2009;27(suppl):1045.